The Geometry of Configuration Spaces for Closed Chains in Two and Three Dimensions

R. James Milgram[†]
Department of Mathematics
Stanford University
Stanford California

Jeff Trinkle[‡]
Department of Computer Science
RPI
Troy, NY

In this note we analyze the topology of the moduli spaces of configurations in the euclidian space $\mathbb{R}^n$ of all linearly immersed polygonal circles with either fixed lengths for the sides or one side allowed to vary. Specifically, this means that the allowed maps of a k-gon $\langle l_1, l_2, \ldots, l_k \rangle$ where the l_i are the lengths of the successive sides, are specified by an ordered k-tuple of points in $\mathbb{R}^n$, P_1, $P_2, \ldots, P_k$ with $d(P_i, P_{i+1}) = l_i$, $1 \le i \le k-1$ and $d(P_k, P_1) = l_k$. The must useful cases are when $n = 2$ or 3, but there is no added complexity in doing the general case. In all dimensions, we show that these configuration spaces are manifolds built out of unions of specific products $(S^{n-1})^H \times I^{n-1-H}$, over (specific) common sub-manifolds of the same form or the boundaries of such manifolds. Once the topology is specified, it is indicated how to apply these results to motion planning problems in $\mathbb{R}^2$.

§1. Introduction

Polygonal circles in $\mathbb{R}^2$ or $\mathbb{R}^3$ with k-edges are called k-bar mechanisms in mechanical engineering, and they often arise with one of the edges fixed. In the latter case they are called closed $(k-1)$-chains. The space of configurations, particularly in the case of closed chains, is very important in areas like robotics where motions of these mechanisms from an initial position to a final position - often with special constraints like avoiding certain points or some self-intersections - are objects of essential interest. We will describe these connections and related problems in §2.
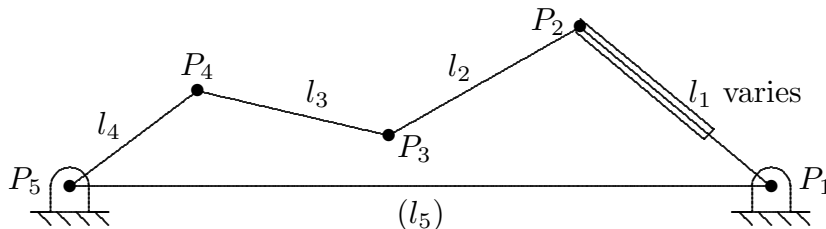

Figure 1: Five bar mechanism with one prismatic joint

1

The Euclidean group of (oriented) rigid motions, $SE_n = \mathbb{R}^n\!:\!SO(n)$, (where $H\!:\!G$ is the semi-direct product and the action of $SO(n)$ on $\mathbb{R}^n$ is the usual one) acts on these configuration spaces. If we mark an edge and initial point on that edge, the action will bring the image of that edge to a fixed segment, say, for definiteness the segment starting at the origin and lying on the positive x_1-axis. This action is not necessarily free in $\mathbb{R}^n$ with $n > 2$ but it is free in $\mathbb{R}^2$. Thus it identifies the configuration space of the k-bar

$$\mathcal{B}(l_1, \ldots, l_k) = \{f\colon \langle l_1, l_2, \ldots, l_k\rangle \longrightarrow \mathbb{R}^2\}$$

in $\mathbb{R}^2$ with a principal fibration

$$\mathbb{R}^2\!:\!SO(2) \longrightarrow \mathcal{B}(l_1, \ldots, l_k) \longrightarrow \mathcal{C}(l_1, \ldots, l_{k-1}|l_k)$$

where $\mathcal{C}$ is the configuration space of an associated closed $(k-1)$-chain with base edge of length l_k.

To describe the moduli spaces of these maps we identify two such maps if and only if they only differ by the action of an element in these oriented affine groups. For configurations of k-bars or closed chains in $\mathbb{R}^3$, after fixing the image of the base edge we still are allowed to rotate the configuration about the line through P_k and P_1. This gives us an S^1 action on the configuration space of the closed chain (which, generically, is free, but is always semi-free, that is to say the orbits are either free or fixed under the S^1-action) with the fixed point set consisting of a finite set of isolated points - those folded chains where all the segments are co-linear. Thus, generically, the projection of the configuration space of a based closed chain in $\mathbb{R}^3$ to the corresponding moduli space is a principal S^1-fibration. A similar situation holds in higher dimensions where the action reduces to an action of SO_{n-1} on the based chains, but this action can have more complex fixed points. (In [KM2] it is shown that in the generic case where the action of $\mathbb{R}^3\!:\!SO(3)$ is free, the quotient manifold has a complex structure. From this it can be shown that the map of the space of configurations where the last edge is mapped to a ray starting at the origin and lying on the positive x-axis to the associated quotient space is a principal S^1-fibration associated to a complex line bundle.)

REMARK 1.1: For $\mathbb{R}^2$ we can extend the action to the group of all rigid motions. In this case, generically, the projection of the configuration space of the closed $(k-1)$-chain to the moduli space is a principal $\mathbb{Z}/2$-fibration.

REMARK 1.2: For all $\mathbb{R}^n$ the configuration spaces depend only on the lengths $l_1, \ldots, l_k$ *and not on their order* up to homeomorphism. Also, in the case where all the lengths are fixed, if we rescale by multiplying all the lengths by the same non-zero constant λ the configuration spaces and moduli spaces are again homeomorphic. Consequently, we can assume that $\sum_1^k l_i = 1$, all the $l_i > 0$, and if we wish, that the lengths are given in increasing order. *Unless otherwise stated this convention will be in force for the remainder of this note whenever we discuss the situation where all the lengths are fixed.*

DEFINITION 1.3: *Assume that the l_i are normalized as above. Then we say that the subset $V = (l_{i_1}, l_{i_2}, \ldots, l_{i_r})$ consists of* **long links** *if and only if the sum of any two lengths in V is greater than $\frac{1}{2}$. The cardinality of V can be at most three.*

The following lemma appears in [KM1] and shows that no real k-bar can have only one long link:

LEMMA 1.4: *The ordered sequence $\langle l_1, l_2, \ldots, l_k \rangle$ with $\sum_1^k l_i = 1$ and $l_i > 0$ for all i, has a non-empty configuration space in $\mathbb{R}^2$ if and only if each $l_i \le \frac{1}{2}$.*

(The proof is elementary. The result is verified for $k = 3$ and then the proof for $k > 3$ is a direct induction when one observes that for $k > 3$, there must be two lengths l_i, l_j with $l_i + l_j < \frac{1}{2}$.)

Sometimes these moduli spaces of configurations will have non-manifold points, but generically, they are manifolds. The conditions for singularity are precisely described in [KM1] and will be reviewed in §4, §5. Here is our first main result.

THEOREM 1.5: *Let $\mathcal{M}$ be a closed $(k-1)$-chain with lengths*

$$l_1, l_2, \ldots, l_{k-1}$$

and base length l_k.

(a) *Except for a finite number of l_k, $\mathcal{C}(\mathcal{M})$ is a closed compact manifold of dimension $(n-1)(k-2) - 1$.*

(b) *Whenever $\mathcal{C}(\mathcal{M})$ is a manifold, it is the boundary of a manifold $W^{(n-1)(k-2)}$ which is given as a union of sub-manifolds of the form*

$$(S^{n-1})^s \times I^{(n-1)(k-2)-s-2},$$

each of which is taut in the sense that its integral homology injects to a direct summand of $H_*(W; \mathbb{Z})$ and the sum of all the images is exactly $H_*(W; \mathbb{Z})$. (The set of s that occur depend on the lengths in a fairly direct way.)
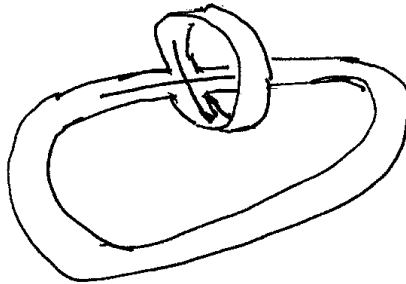

Figure 2: The (coordinate) union of two copies of $S^1 \times I$

This union is constructed as follows. Whenever two such pieces intersect, their intersection is a common (coordinate) sub-manifold of the form $(S^{n-1})^l$ with trivial normal bundle and

3

a certain number of the coordinates in the normal bundle point in the direction of the first piece, while a complementary set point in the direction of the second. Also, any two of these sub-manifolds have at least one point in common, $(S^{n-1})^0$.

Here, coordinate sub-torus simply means that we fix a finite number of the product coordinates in $(S^{n-1})^{k-1}$ and allow the remaining points to vary over all possible values. Also, the structure of this finite union of sub-tori (shorthand for products of spheres) is entirely explicit, consisting of a finite number of maximal sub-tori together with *all their possible intersections*, and the set of maximal sub-tori is given in the body of the paper as a combinatorial function of the lengths.

REMARK 1.6: In specific cases, it is quite direct to determine the exact structure of these W^m.

EXAMPLES 1.7: We give some examples for $\mathbb{R}^2$.
(a) If all the l_i, $i < k$, are equal, then the only possible W^{k-2} are thickenings of the full s-skeleton of $(S^1)^{(k-1)}$ for $s \leq [(k-1)/2]$. Compare [K1], [KTT], [KT], which use very different techniques.
(b) If there are three long edges, the thickening is

$$(S^1)^{k-3} \times I.$$

(c) If there are two long edges, the space $\mathcal{C}(\mathcal{M})$ is the double over the boundary of one of these thickenings.
(d) In the general case $\mathcal{C}(\mathcal{M})$ is the double over the boundary of the difference between two of these thickenings:
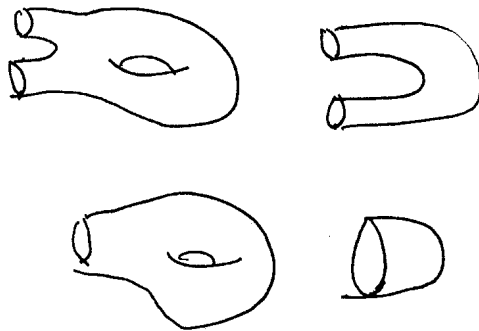

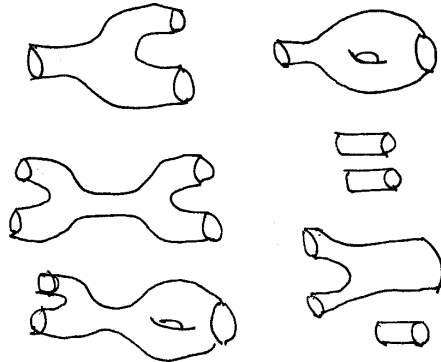**Figure 3: Thickenings with boundaries $\mathcal{C}$-spaces for 4-bars**

Figure 4: The differences of the thickenings above

Moreover, from the description above, the intersection pairing is easily described in any specific case, so the homology structure of the $\mathcal{C}(\mathcal{M})$ can be regarded as completely known for any closed chains in $\mathbb{R}^2$ with no obstacles.

These thickenings are also the building blocks for constructing the configuration spaces themselves in the case of $\mathbb{R}^2$. In fact, the configuration spaces for fixed-length mechanisms are simply doubles along the boundary of a certain associated W^{k-2} or the difference of two such, W^{k-2} and $W'^{(k-2)} \subset W^{k-2}$. On the other hand, these differences are *precisely* the configuration spaces of mechanisms where the length of exactly one edge is allowed to vary between two finite values, i.e., a mechanism with one *prismatic* joint,

$$0 \leq l(0) \leq l_n \leq l(1) \leq \sum_1^{k-1} l_j.$$

THEOREM 1.8: *Let $n = 2$. Suppose all the edges have fixed length, suppose that the assumptions of the above theorem are satisfied, and suppose, moreover, that there are two "long edges", l_i and l_j, $(i \neq j)$, so that $l_i + l_j > \frac{1}{2}$. Then the configuration space for the associated k-bar mechanism is the double along the boundary of a thickening having the type described in the previous theorem for $\mathbb{R}^2$.*

REMARK 1.9: The descriptions of the associated configuration spaces in $\mathbb{R}^n$ are somewhat more complicated, though they are still doubles.

REMARK 1.10: It is also possible for the mechanism to have three long edges l_i, l_j, l_k so that the sum of any two is $\geq \frac{1}{2}$, though it is not possible to have four long edges. In the case of three long edges we have the important result, [KM1]:

THEOREM 1.12: *For configurations of an k-bar mechanism with fixed lengths in $\mathbb{R}^2$ the configuration space is connected if and only if the mechanism does not have three long*

edges. Moreover, in the case where the mechanism does have three long edges, then the configuration space has exactly two components and each component is a torus $(S^1)^{k-3}$. (In $\mathbb{R}^n$, $n \geq 3$, the moduli space is always connected.)

The explicit descriptions of the configuration spaces given above allow for very efficient motion planning in these thickened regions or differences of thickened regions. Specifically, when the topology of the region is sufficiently well understood, it is possible to construct efficient (piecewise geodesic with very few breaks) paths in polynomial time, (roughly vk^4) where v is a constant that depends on the specific configuration space.

Also, the determination of the relevant aspects of the topology of these regions can be done in roughly 2^{3k} steps (which is best possible in general, though when there are very few distinct lengths, the number is much smaller). Of course, this latter calculation need only be done once.

The authors have used these results to develop a *complete* program for motion planning for closed chains that works in polynomial time independent of whether the topology is well understood. The trade off is that these paths may be quite far from optimal. (Here complete means that if it is possible to find a path from the initial configuration to the final configuration, the program will construct one, and if it is not possible, the program will report this as well.)

These closed k-chains are a special family of linkages. Over the years, quite a number of papers have been written that deal with aspects of the problem of determining the configuration spaces and moduli spaces of linkages. It is known, as was shown by Thurston (unpublished, but see [KM3]), that the complexity of the full subject is that of real algebraic geometry, though, as the results above show, the situation becomes much more manageable when we restrict to special families. Recently the results of [KM1], [KM2], [KM3], provide a good review of previous work and give a number of interesting results on the structure of these configuration spaces, particularly the configuration spaces for closed chains in $\mathbb{R}^2$ and $\mathbb{R}^3$.

Worth special note is the work of J. C. Hausmann, and J. C. Housmann with A. Knutson [Ha], [HK] who determine the cohomology rings of a number of these spaces but not their detailed homotopy types. Also one should note the work of Y. Kamiyama and a number of collaborators [K1], [K2], [K3], [KTT], [KT] who study the case where all the edge lengths or all the edge lengths but one are the same by different methods.

In further work, the present authors expect to discuss extensions of the results above to configuration spaces for closed chains in the presence of obstacles and constraints. Also, we would like to thank Steven Kaufman for all the help and encouragement he gave us throughout the development of these results.

§2: Background

Kinematics is the study of the possible motions of systems of bodies coupled mechanically through contact constraints. These constraints can be permanent, as in the case of a hinge joint, or intermittent, as in the case of a ratchet mechanism. A common problem in mechanism design is to choose the number of links and their lengths, twists, and offsets, so as to allow a particular link to move (relative to a given base link) from one configuration to another, possibly following some specified rigid body motion. Currently, this design problem is solved taking little or no advantage of the structure of the space of configurations of the mechanisms under consideration. While some research results that leverage global structure of the configuration spaces have appeared in the literature [†], common design practices still tend to rely on iterative numerical procedures that use only local information. As a result, the design process for mechanisms with even small numbers of joints is tedious.

In the design of common one-degree-of-freedom mechanisms, such as the four-bar linkage and crank and slider mechanisms, [H], current design tools are reasonably powerful and efficient. However, the field of robotics has been placing increasingly difficult demands on mechanism designers. Most robotic applications require more degrees of freedom from mechanisms than current design tools can readily handle. One challenging class of robotics problems requires the motion planning and control of a closed-chain mechanism with many degrees of freedom. For example, a bomb-disposal robot must be capable of moving to a door (behind which is a bomb), and opening it. While the robot is opening the door, a closed kinematic chain is formed that is composed of the robot arm and the door, connected to the ground at either end. To open the door, one must understand the constraints imposed on the system by the kinematic loop and be able to plan the motion of the system from an initial state (the door is closed) to a goal state (the door is fully open).

Despite the fact that bomb-disposal and many other robotic tasks require good designs and motion planning for closed kinematic chains, the state of the art is surprisingly crude. The most effective robot motion planners today are built upon randomized search techniques. [KLOS], [WXH]. However, individual randomized techniques have wildly varying performance and are not complete; they are not guaranteed to find a solution when one exists, nor can they determine that a solution does not exist when that is the case. The theoretical basis for a complete general motion planner was developed roughly 15 years ago, [C], but it has never been implemented due to the complexity of the specified algorithms.

The work presented here represents a first step in the development of maximally efficient, complete motion planners for robotic mechanisms. More importantly, the work

---

[†] For example, Shukla and Mallik, [SM], developed a method to determine the existence of a crank (a link that can rotate 360° relative to some other link in Watt and Stephenson chains (six-bar, planar mechanisms with two loops)).

expands the field of theoretical kinematics. Previously, the only mechanisms for which the global properties of configuration space were understood, were those of planar mechanisms with very small numbers of joints (e.g., the four-bar mechanism). Here we completely determine the global structure of configuration spaces of spatial n-bar mechanisms, where n is arbitrary. The class of mechanisms considered are those forming a single closed loop. For planar mechanisms, all joints are of the type know as "revolute" (i.e., hinge joints); they constrain adjacent links in the loop allowing only relative rotation about the axis of the joint. For spatial mechanisms, all links are connected by "U"-joints (i.e., pairs of revolute joints with intersecting axes). In addition, one link is allowed to change its length (i.e., the mechanism may have one prismatic joint). While our analysis allows self-intersection of the links, once the associated configuration space is understood, there are standard methods in topology for dealing with restrictions on the embeddings so that, for example, there are no self-intersections or the mechanisms do not intersect given closed sets in $\mathbb{R}^2$ or $\mathbb{R}^3$. We will not discuss these techniques here, but expect to do so in subsequent work.

§3: Planning Paths in the Configuration Space

Briefly, assume that we are given two points, A and B, in the configuration space of a closed chain in $\mathbb{R}^n$, with the last edge based at $\vec{0}$ and lying on the x_1-axis. Then the space of paths from A to B is homotopy equivalent to the loop-space $\Omega(\mathcal{B}(l_1, \ldots, l_k))$ (if A and B lie in the same path-component) or it is empty. Consequently, for $k > 4$, if the loop space is not empty, then there are many ways of moving from A to B. Given the non-uniqueness of paths and the huge difficulty, in general, of determining geodesics between A and B, one must identify the most important path attributes to guide their construction.

If any path between A and B will do, then one may proceed a step at a time. Using 1.12, we can check whether we are dealing with a path connected space or one that has two components. If there are two components, then they are distinguished by the relative positions of the three long links. For example, if the long links are l_2, l_3 and l_4 (as in Figure 5), then $\{l_2, l_3\}$ will be in one half-plane or the other relative to l_4.
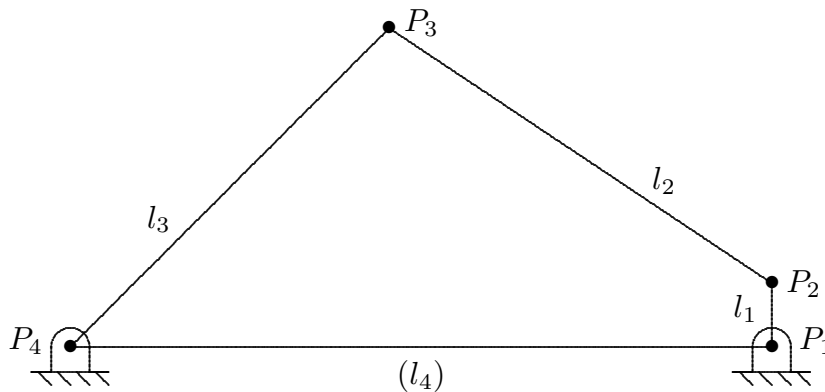

Figure 5: A four-bar mechanism with three long links.

Since in the case of two components, the short links are free to move in any way, the configuration space is comprised of two tori. Hence the motion planning algorithm here is very simple, determine if A and B are in the same component and, if so, move the short links in a straight line on the torus from their configuration for A to their configuration for B.

In the case of a single path connected component, one can simply move one link after another into the correct position, and then fix it. Having fixed a link, we can lump it with the old base link to form a new base link leaving a closed chain with one less link. The next move will be from the configuration just achieved, A_k, to the original goal configuration, B. Before beginning the next move, however, one checks the number of components in configuration space of the reduced chain. If there are two components and A_k and B are in the same component, proceed as in the previous paragraph. If they are not in the same component, we adjust the previous move to ensure that the long links move into the correct relative position before moving the next link into its correct final position.

Such algorithms take advantage only of our knowledge of the path components and our ability to detect which component contains a given configuration. But we also know much more about the geometry and topology of the configuration space than just the components. It turns out that the tori $(S^{n-1})^s \times pt \subset (S^{n-1})^s \times I^{(n-1)(k-s-2)}$ in our W's are very close to geodesic, so when design constraints permit, it is quite efficient to locate one of these tori close to A, another close to B. This done, one can plan the path by constructing a path in the poset of the $(S^{n-1})^s$ from the first torus to the other. Of course, this requires that one do a potentially very long analysis of a certain set of critical radii given explicitly in the statement of 5.1. Algorithms for doing this can be extracted from the discussion that follows 7.8.

§4: Constructing Configuration Spaces of Closed Chains

In this section we restrict ourselves to $\mathbb{R}^2$. It is direct to extend the discussion to $\mathbb{R}^n$ however, and we indicate the key changes as we procede. Also, before we do the analysis of the closed situation, we consider open chains (where one end-point is allowed to vary but the other is fixed).

For open chains the structure of the configuration space is clear: a chain's configuration is determined by the successive angles between the edges, and between the base edge and some fixed ray emanating from the base-point. Consequently, the configuration space of an open chain with k segments is just the k-torus $(S^1)^k$, (for $\mathbb{R}^n$, the product $(S^{n-1})^k$).

We also need to consider the workspace of an open chain. This consists of all the points in the plane that occur as the image of the free end-point of the chain. For example, in the case of an open chain with two unequal edges the workspace is always an annulus centered at the fixed end-point, with outer circle of radius $l_1 + l_2$ and inner circle of radius $|l_1 - l_2|$.

(In $\mathbb{R}^n$ it is a product $S^{n-1} \times I$ having the same inner and outer radii.)
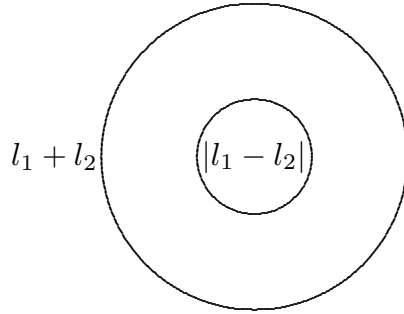

Figure 6: Annular Workspace for Two-Edge Linkage

Here, it is also worth noting that there are exactly two configurations with a given end-point as long as the end-point is in the interior of the annulus, while the configurations on the boundary circles occur only when the two edges lie on a *single* line through the base-point. In the case where the two edges have equal length the workspace is the entire disk of radius $2l_1$, but the inverse image of the base-point in the configuration space consists of an entire circle.

In the case of an open chain with a single edge of length l, the workspace is just the circle of radius l centered at the base-point, while the workspace for a general open chain with at least three links is either the closed annulus or the closed disk centered at the origin. In both cases the outer radius will be $\sum_i l_i$.

Let us consider the configuration space of *closed chains* with three segments, i.e., planar 4-bar mechanisms. To do this we consider simultaneously an open chain with one edge of length l_3 based at P_4 and an open chain with two edges of lengths l_1 and l_2, based at P_1. Assume, for the moment that P_1 and P_4 are further apart than $l_1 + l_2 + l_3$, so there is no configuration of the closed chain that connects P_1 and P_4. Then start moving P_4 towards P_1 till the edges of the workspaces touch as shown in Figure 7:
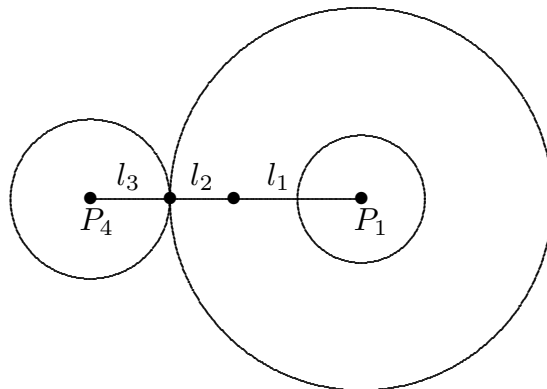

Figure 7: Workspaces Just Touching

Now there is a single solution – the three edges lie along the line containing P_1 and P_4. Continue to move P_4 towards P_1, so the intersection of the workspaces is an arc whose

10

interior is completely contained in the interior of the annular workspace of the 2-chain. (In $\mathbb{R}^n$, $n \geq 3$, the intersection is a disc $D^{n-1} \subset S^{n-1}$.) At each interior point $\vec{v}$ of the arc there are exactly two configurations of the 2-chain at P_1 with $\vec{v}$ locating the free end-point. (In $\mathbb{R}^n$, $n \geq 3$ the configurations form an S^{n-2} at each interior point of the D^{n-1}.) At each end-point of the arc there is only one configuration of the 2-chain both in $\mathbb{R}^2$ and $\mathbb{R}^n$ with $n \geq 3$. Consequently, for the region defined by

$$l_1 + l_2 > ||P_1 - P_4|| - l_3 > |l_1 - l_2|$$

(provided that $||P_1 - P_4|| > l_1 + l_2 - l_3$) the configuration space is simply a circle for $n = 2$, more generally and S^{n-1}. (Four-bar mechanisms satisfying the condition that their configuration space is a single circle are referred to as *non-Grashof* in the engineering literature.)

The configuration space continues to be a circle, (S^{n-1}), as P_4 moves towards P_1 until either the arc of intersection touches the interior circle of the annulus (or P_1 when the interior circle is degenerate, *i.e.*, $l_2 = l_1$), (which will occur if $2l_3 > |l_1 - l_2|$)
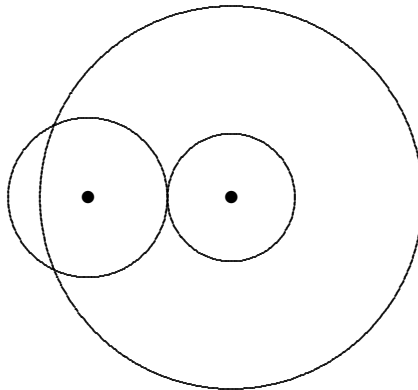
Figure 8: Workspaces Just Touching at Inner Boundary

or the intersection becomes the entire circle, with one point tangent to the outer circle of the annulus (which can only happen if $2l_3 < |l_1 - l_2|$). Mechanisms with this type of configuration space are known in the engineering literature as *uncertain* since the inverse image of motion through the singular point given by three colinear links bifurcates.

Figure 9: Workspace Contained and Touching Outer Boundary

11

In both these cases the configuration space becomes a figure 8, while in the degenerate case (occurring when $2l_3 = |l_1 - l_2| > 0$), we find that the configuration space becomes the following graph:
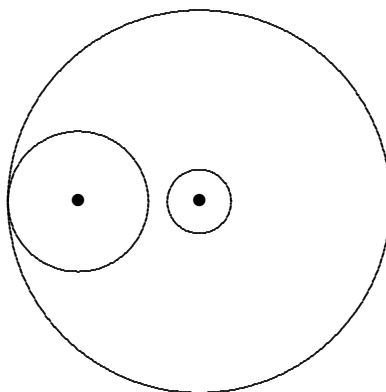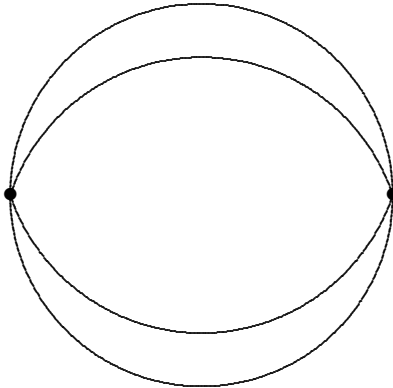

Figure 10: Three Loop Graph With Two Vertices

The remaining case occurs when the arc becomes tangent to the inner and outer circles of the annulus simultaneously *and*, the inner circle degenerates to the point P_1, *i.e.*, $l_1 = l_2 = l_3$. In this case the configuration space is a three vertex, six edge graph, with four edges incident on each vertex.

As P_4 continues to move towards P_1 various possibilities now occur. The two most important are represented in continuing the situations in both Figure 8 and Figure 9, where, in two different ways - as the circle crosses the inner radius in Figure 8, or becomes entirely contained in the interior of the annulus for Figure 9 - the configuration space becomes two disjoint circles. In the engineering literature, this is referred to as *Grashof*, and represents the usual way in which four-bar mechanisms are applied. (Here is where the situation starts to significantly deviate between $\mathbb{R}^2$ and $\mathbb{R}^n$, $n \geq 3$. For example, the generic situation for $\mathbb{R}^3$ is the sequence S^3, $S^1 \times S^2$, S^3, $\mathbb{RP}^3$, while the corresponding sequence for $\mathbb{R}^2$ is S^1, $S^1 \sqcup S^1$, S^1, $S^1 \sqcup S^1$.)

The reader can easily list the remaining possibilities. A similar analysis can be done for five bar mechanisms, and such an approach is discussed in [KM1]. There are exactly six non-singular closed surfaces that appear as configuration spaces for 5-bar mechanisms in $\mathbb{R}^2$, the surfaces of genus ≤ 4 and the disjoint union of two copies of the torus $S^1 \times S^1$. However, as the number of bars increases, this approach becomes too complex, and we need more systematic and powerful methods. (This is already evident for the 4-bar mechanisms in $\mathbb{R}^n$, $n \geq 3$ as the previous paragraph indicates.)

§5: Generic points for the map to the workspace

The considerations above indicate that it should be possible to "bootstrap" from k-bars to $(k + 1)$-bars, provided we understand the entire configuration space for the

lengths $l_1, l_2, \ldots, l_{k-1}$ in the sense that we know the inverse image of any point in the workspace. In doing this, we introduce the intersection of the circle of radius l_k and the workspace, provided that the center of this circle is at distance l_{k+1} from the origin. Then the configuration space of the $(k + 1)$-bar is the inverse image of this intersection.

Also, the considerations above indicate that there are certain critical circles, (spheres S^{n-1} for $\mathbb{R}^n$), in the workspace, those circles where the inverse image contains a configuration with all the edges colinear, and that the inverse image will be non-singular unless the circle of radius l_k is *tangent* to one of these critical circles.

Both of these results are true. In fact, even more is true. If we choose an initial point on the circle and take the (signed) distance on the component of the intersection of the circle of radius l_k with the workspace that contains the initial point, as a function on the inverse image of the configuration space, then this function is *locally* Morse, with all its critical points contained in the inverse images of the intersection of this circle with the critical circles in the workspace.

Here are the basic results.

THEOREM 5.1: *Let $\vec{q}$ be any point in the workspace of the open chain with lengths*
$$\langle l_1, l_2, \ldots, l_k \rangle,$$
then the inverse image of a point p in the torus $(S^{n-1})^k$ is an $(n-1)(k-1)-1$ dimensional manifold if and only if p is not on one of the circles (spheres), centered at the center of the workspace having radius $R_I = |\sum l_i - 2\sum_{j \in I} l_j|$ where $I \subset \{1, 2, \ldots, n\}$ is any subset.

THEOREM 5.2: *Suppose that γ is a rectifiable curve embedded in the workspace and $\vec{0} \notin \gamma$. Then the inverse image of γ is non-singular if and only if γ is transverse to each of the critical circles (spheres) that it intersects.*

(Here the critical circles and spheres are the spheres described in the result above.)

COROLLARY 5.3: *Let R_I and R_J be adjacent critical radii, and $W(I, J)$ the open annulus (in $\mathbb{R}^2$) or open spherical shell (in $\mathbb{R}^n$) between them, then the map of the inverse image of $W(I, J)$ onto $W(I, J)$ is a fibration.*

REMARK: The exact structure of this fibration will be clarified in 6.5. There is an action of SO_n on $W(I, J)$ defined in 6.3 with the key property 6.4 that enables us to define these fibrations as bundles associated to the restricted action of SO_{n-1} on the space $e^{-1}(w)$ for some $w \in W(I, J)$. Such bundles are generically non-trivial, but are trivial over any curve in $W(I, J)$ for $n \geq 2$.

As a consequence, if the curve γ lies entirely in one of the $W(I, J)$, then the inverse image of γ is also a product $I \times V$ where V is the inverse image of an arbitrary point in $W(I, J)$, and it follows that any two embedded γ which lie entirely in $W(I, J)$ have diffeomorphic inverse images.

THEOREM 5.4: *Suppose that the curve γ in the workspace satisfies the properties above for non-singularity of the inverse image. Then arc length on γ is locally a Morse function on the inverse image, W, of γ, with critical points exactly the points in W intersected with the critical circles (spheres) where all the edges are co-linear.*

In the next two sections we give the proofs.

§6: The proofs of the general position theorems above

LEMMA 6.1: *The map e which sends an open chain with lengths $l_1, \ldots, l_k$, based at 0 to its endpoint has the following properties:*

(a) *It is real algebraic.*

(b) *The singular points of e are precisely the $(n-1)$-spheres $(\vec{X}_1, \vec{X}_2, \ldots, \vec{X}_k)$ in the configuration space $(S^{n-1})^k$, where all the $\vec{X}_j$ are parallel, (so $\vec{X}_j = (-1)^{\epsilon_j} \vec{X}_1$, $j = 2, \ldots, k$).*

(c) *e maps the singular set diffeomorphically onto a collection of spheres S^{n-1} centered at the origin of radii $|l_1 + \sum_{i=2}^{k}(-1)^{\epsilon_i} l_i|$ where the $(k-1)$-tuples $(\epsilon_2, \ldots, \epsilon_k)$ run over all $2^{(k-1)}$ possibilities with each $\epsilon_i \in \{0, 1\}$.*

EXAMPLE 6.2: *If $(l_1, l_2, l_3, l_4) = (1, 1.5, 2, 3)$ then there are exactly six critical radii, .5, 1.5, 2.5, 3.5, 4.5 and 7.5 with 1.5 and 2.5 occurring in four distinct ways, and each of the others in 2 distinct ways.*

PROOF: S^{n-1} is real algebraic, so $(S^{n-1})^k$ is as well. Moreover, the map e is given explicitly as

$$e(\vec{X}_1, \ldots, \vec{X}_k) = \sum_{1}^{k} l_i \vec{X}_i,$$

and is consequently real algebraic.

We now consider the tangent map $d(e)$. The tangent space to $(S^{n-1})^k$ at $(\vec{X}_1, \ldots, \vec{X}_k)$ is the direct sum

$$\tau_{\vec{X}_1}(S^{n-1}) \oplus \tau_{\vec{X}_2}(S^{n-1}) \oplus \cdots \oplus \tau_{\vec{X}_k}(S^{n-1}),$$

and $d(e)$ is just $l_i \times I$ on $\tau_{\vec{X}_i}(S^{n-1})$, where I is the inclusion $\tau_{\vec{X}_i}(S^{n-1}) \subsetneq \tau_{\vec{X}_i}(\mathbb{R}^n)$ as the vector subspace $\vec{X}_i^{\perp}$. Clearly, since $\vec{X}_i^{\perp}$ has codimension 1 in $\mathbb{R}^n$, unless all these subspaces are the same, the subspace of

$$\tau_{e(\vec{X}_1, \ldots, \vec{X}_k)}(\mathbb{R}^n)$$

14

spanned by these subspaces will be $\tau_{e(\vec{X}_1,\ldots,\vec{X}_k)}(\mathbb{R}^n)$ itself, and the point will be non-singular for e. But when all the images are the same, then $\vec{X}_1^{\perp}$ will be the image of $d(e)$ and the point will be singular. ∎

Standard results for C^∞ maps with compact inverse images of points show that e is a fibration in any connected component of $e((S^{n-1})^k) - Im(Sing(e))$. Consequently this is the case for each annular region between two successive critical spheres. To understand these fibrations we need the action of O_n on $(S^{n-1})^k$ defined by

6.3
$$g(\vec{X}_1,\ldots,\vec{X}_k) \;=\; (g(\vec{X}_1),\ldots,g(\vec{X}_k)),$$

for $g \in O_n$. A key property of this action is that

$$g(e(\vec{X}_1,\ldots,\vec{X}_k)) \;=\; e(g(\vec{X}_1),\ldots,g(\vec{X}_k))$$

so we have the commutative diagram

6.4
$$
\begin{array}{ccc}
(S^{n-1})^k & \xrightarrow{\;g\;} & (S^{n-1})^k \\
\downarrow{\scriptstyle e} & & \downarrow{\scriptstyle e} \\
\mathbb{R}^n & \xrightarrow{\;g\;} & \mathbb{R}^n
\end{array}
$$

for each $g \in O_n$. As a consequence, if $e(\vec{X}_1,\ldots,\vec{X}_k) = \vec{Y}$ with $\vec{Y} \neq \vec{0}$ and $O_{n-1}(\vec{Y})$ is the subgroup of O_n that fixes $\vec{Y}$. It follows that $O_{n-1}(\vec{Y})$ *acts* on $e^{-1}(\vec{Y})$ by restriction. Also, note that $O_{n-1}(\vec{Y})$ is conjugate to the usual $O_{n-1} \subsetneq O_n$.

As an example, when $k = 2$ we know that for any point $\vec{Y}$ in the interior of the image of e, $e^{-1}(\vec{Y}) = S^{n-2}$, and O_{n-1} acts in the usual way on $S^{n-2} \subsetneq \mathbb{R}^{n-1}$. In this case, the fibration is given as the associated fiber bundle with total space

$$S^{n-2} \times_{O_{n-1}} O_n \cong S^{n-2} \times_{SO_{n-1}} SO_n$$

and projection
$$\pi : S^{n-2} \times_{SO_{n-1}} SO_n \longrightarrow SO_{n-1}\backslash SO_n = S^{n-1}$$

when restricted to any orbit sphere S^{n-1} of O_n in V. This is the *the tangent bundle to* S^{n-1} and is non-trivial for $n \neq 2, 4, 8$, [A].

More generally, if $N = e^{-1}(\vec{Y})$ for $\vec{Y} \neq 0$ with $\vec{Y} \in Im(e)$, and k, n arbitrary, then we can describe $e^{-1}(V)$ as the product bundle

$$Id \times \pi : I \times \left(N \times_{SO_{n-1}} SO_n\right) \longrightarrow I \times (SO_{n-1}\backslash SO_n) = I \times S^{n-1}$$

associated to the SO_{n-1} action on N.

15

COROLLARY 6.5: *Let V be the open annular region between two successive critical spheres in the situation above. Then the inverse image of V is a fibration over V. The fibration is trivial, $V \times e^{-1}(V)$ if $n = 2$, but is usually non-trivial for $n \geq 3$.*

Let γ be any rectifiable curve embedded in the workspace, and suppose that W is the inverse image of γ under e.

COROLLARY 6.6: *Suppose that γ does not contain $\vec{0}$. Then W is a differentiable manifold if and only if γ intersects each critical sphere transversally. Moreover, if γ satisfies these assumptions, then the set of critical points of the composition of the length function on γ with e on W is exactly the set of $(\vec{X}_1, \ldots, \vec{X}_{n-1}) \in W$ where all the $\vec{X}_i$ are colinear.*

PROOF: Under these assumptions the map e is transverse regular at every point of γ, and this implies that the inverse image of γ, $e^{-1}(\gamma) = W$, is a differentiable manifold.

It is clear that de restricted to $\tau_v(W)$ is onto $\tau_{e(v)}(\gamma)$ except possibly when v is contained in the singular set of e. What needs to be checked is that $de : \tau_v(W) \rightarrow \tau_{e(v)}(\gamma)$ is the 0-map whenever $v \in Sing(e) \cap W$. But since γ is transverse to $Im(Sing(e))$ at such a v, and the image of $de(\tau_v((S^{n-1})^i) \subset \tau_{e(v)}(Im(Sing(e)))$, it follows that the image of $de|\tau_v(W)$ must be $\vec{0}$ in $\tau_{e(v)}(\gamma)$. ∎

Thus we have shown that under the assumptions above, the length function $s_\gamma f$ restricted to W has isolated critical points. It remains to analyze the Hessian at these critical points to prove that this function is Morse.

A KEY EXAMPLE: The curve we will study now is $\gamma = \begin{pmatrix} t \\ 0 \\ \vdots \\ 0 \end{pmatrix}$ in a neighborhood of the

singular image $\begin{pmatrix} |\sum_1^k (-1)^{\epsilon_i} l_i| \\ 0 \\ \vdots \\ 0 \end{pmatrix}$. Let W be the inverse image of γ for t in the interval

$$(|\sum_1^n (-1)^{\epsilon_i} l_i| - \delta, |\sum_1^n (-1)^{\epsilon_i} l_i| + \delta)$$

with $\delta > 0$ appropriately small. On this W we have that the arc-length function is simply the first coordinate of γ, t up to adding an appropriate constant.

In a neighborhood of the critical point in W we have the following points in the

configuration space

$$
\left((-1)^{\epsilon_1} \begin{pmatrix} \sqrt{1 - m_{12}^2 - \cdots - m_{1n}^2} \\ m_{12} \\ \vdots \\ m_{1n} \end{pmatrix}, \cdots, (-1)^{\epsilon_k} \begin{pmatrix} \sqrt{1 - m_{k2}^2 - \cdots - m_{kn}^2} \\ m_{k2} \\ \vdots \\ m_{kn} \end{pmatrix} \right)
$$

and the constraints that they lie in W are $\sum_1^k l_j m_{js} = 0$ for $2 \leq s \leq n$. It follows that we can take the m_{js}, $2 \leq s \leq n$, $2 \leq j \leq k$ as local coordinates in W near the critical point. In terms of these coordinates, the terms $m_{12}, \ldots, m_{1n}$ are given by

$$
m_{1i} = (-1)^{\epsilon_1 + 1} \sum_2^k (-1)^{\epsilon_j} \frac{l_j}{l_1} m_{ji}, \text{ for } 2 \leq i \leq n.
$$

Also, the arc-length function is given in the form

6.7
$$
f(m_{22}, \ldots, m_{kn}) = \sum_{i=1}^k (-1)^{\epsilon_i} l_i \sqrt{1 - m_{i2}^2 - \cdots - m_{in}^2},
$$

up to adding an appropriate constant.

The partial derivatives are

$$
\begin{aligned}
\frac{\partial f}{\partial m_{ij}} &= (-1)^{\epsilon_1 + 1} l_1 \frac{m_{1j}}{\sqrt{1 - m_{12}^2 - \cdots - m_{1n}^2}} \frac{\partial m_{1j}}{\partial m_{ij}} + (-1)^{\epsilon_i + 1} l_i \frac{m_{ij}}{\sqrt{1 - m_{i2}^2 - \cdots - m_{in}^2}} \\
&= (-1)^{\epsilon_i} \frac{m_{1j}}{\sqrt{1 - m_{12}^2 - \cdots - m_{1n}^2}} l_i + (-1)^{\epsilon_i + 1} l_i \frac{m_{ij}}{\sqrt{1 - m_{i2}^2 - \cdots - m_{in}^2}}
\end{aligned}
$$

and they are, as expected, all 0 at the point $m_{ij} = 0$, $2 \leq i \leq k$, $2 \leq j \leq n$. Similarly, the second derivatives $\frac{\partial^2 f}{\partial m_{ij} \partial m_{vw}}$ are 0 unless $w = j$, and

6.8
$$
\frac{\partial^2 f}{\partial m_{ij} \partial m_{vj}} = (-1)^{\epsilon_1 + \epsilon_i + \epsilon_v + 1} \frac{l_i l_v}{l_1} + \delta_{v,i} (-1)^{\epsilon_i + 1} l_i
$$

in the case where $w = j$. Here $\delta_{v,i} = \begin{cases} 0 & \text{if } v \neq i \\ 1 & \text{if } v = i. \end{cases}$. Thus the Hessian matrix, H, of second partial derivatives is a block diagonal matrix of the form

$$
H = \begin{pmatrix} D & 0 & 0 & \ldots & 0 \\ 0 & D & 0 & \ldots & 0 \\ 0 & 0 & D & \ldots & 0 \\ \vdots & \vdots & \vdots & \ddots & \vdots \\ 0 & 0 & 0 & \ldots & D \end{pmatrix}
$$

17

with D a $(k-1) \times (k-1)$ matrix and $(-1)^{\epsilon_1+1} l_1$ multiplied by the $i-1, v-1$ term of D equal to

$$(-1)^{\epsilon_i+\epsilon_v} l_i l_v + \delta_{i,v}(-1)^{\epsilon_1+\epsilon_i} l_i l_1.$$

Consequently, D is the sum of the diagonal matrix

$$C \;=\; (-1)^{\epsilon_1+1}\frac{1}{l_1}
\begin{pmatrix}
(-1)^{\epsilon_2+\epsilon_1} l_1 l_2 & 0 & 0 & \cdots & 0 \\
0 & (-1)^{j(3)} l_1 l_3 & 0 & \cdots & 0 \\
0 & 0 & (-1)^{j(4)} l_1 l_4 & \cdots & 0 \\
\vdots & \vdots & \vdots & \ddots & \vdots \\
0 & 0 & 0 & \cdots & (-1)^{\epsilon_k+\epsilon_1} l_1 l_k
\end{pmatrix}$$

and the rank 1 matrix

$$RR^t \;=\; (-1)^{\epsilon_1+1}\frac{1}{l_1}
\begin{pmatrix}
l_2^2 & (-1)^{\epsilon_2+\epsilon_3} l_2 l_3 & \cdots & (-1)^{\epsilon_2+\epsilon_k} l_2 l_k \\
(-1)^{\epsilon_2+\epsilon_3} l_2 l_3 & l_3^2 & \cdots & (-1)^{\epsilon_3+\epsilon_k} l_3 l_k \\
\vdots & \vdots & \ddots & \vdots \\
(-1)^{\epsilon_2+\epsilon_k} l_2 l_k & (-1)^{\epsilon_3+\epsilon_k} l_3 l_k & \cdots & l_k^2
\end{pmatrix}$$

where $R^t = ((-1)^{\epsilon_2} l_2, \ldots, (-1)^{\epsilon_k} l_k)$. Since RR^t is rank 1, it follows that all the $s \times s$ minors of RR^t are 0 for $k-1 \geq s \geq 2$. From this it is direct that

$$Det(D) \;=\; \pm \frac{1}{l_1} \prod_2^k l_j \times \left(\sum_1^k (-1)^{\epsilon_j} l_j \right)$$

is non-zero. We have verified that f is Morse on this special γ.

We now complete the proofs of our main theorems by showing that this special case implies the general case.

So let $v \in W \cap Sing(e)$ have image μ contained in the sphere of radius $\sum_1^k (-1)^{\epsilon_i} l_i$ about $\vec{0}$. Let $\mu \in \gamma = e(v)$. Then there is an open neighborhood of $e(v)$ in γ, N so that

(1) at most one point in N has distance t from the origin (from the fact that N is transverse to the sphere of radius $\sum_1^k (-1)^{\epsilon_i} l_i$),

(2) there is a C^∞ map $\lambda \colon N \to SO_n$ so that for each $v \in N$, $\lambda(v)(v)$ is contained in the curve $\begin{pmatrix} t \\ 0 \\ \vdots \\ 0 \end{pmatrix}$ above.

The corresponding action of $\lambda(N)$ on $e^{-1}(N) = W_1$, (defined in 6.3), gives a diffeomorphism from $e^{-1}(N)$ to $e^{-1}(\lambda(N))$, (because of 6.4), and the original arc-length function on N is a composition $h \circ f \circ \lambda$ with $\frac{dh}{dt} \geq 1$ at the image of v. But from this, the Hessian

18

with respect to arc-length on γ is the same as the Hessian on the sample curve above multiplied by $\frac{dh}{dt}$ evaluated at $\mu(e(v))$. This completes the proof of our main technical assertion, Theorem 5.4.

§7: The structure of inverse images of curves

It turns out that we do not need the exact index of these critical points. What matters is how many of them there are in the inverse image of a given path in the workspace. But before we get into these details we need to make a few remarks about the dependence of these inverse images on the particular path, γ.

Throughout this section we assume that the inequalities among the $l_1, \ldots, l_n$ required for the non-singularity of all the critical points are satisfied.

By assumption γ is differentiable and has transverse intersections with the critical point spheres of the map from the free configuration space to the workspace. Assume that γ has been parameterized by (scaled) arc-length and is thus given by a unique differentiable map $I \rightarrow e(W(l_1, \ldots, l_n))$. It follows that the union of these intersection points forms a discrete labeled configuration of points in I, where the labeling is by the radius of the particular critical sphere containing the image. Clearly, there is a single constraint on this set - adjacent labeled points must either be labeled by the same radius or by the next larger or smaller radius. But aside from this constraint any finite, discrete configuration of labeled points can arise. We call the resulting labeled configurations that actually arise *admissible configurations*. All the admissible configurations are naturally *ordered* via the natural ordering of the inverse images of the critical spheres in I, and thus, associated to each admissible configuration there is a unique ordered sequence of radii of critical spheres.

DEFINITION 7.1: *Two admissible configurations are equivalent if and only if the associated ordered sequences of radii of critical spheres are equal.*

The following result is now direct from 5.3.

THEOREM 7.2: *Let γ_1 and γ_2 be two admissible curves in the workspace $W(l_1, \ldots, l_n)$ with the same end-points which are not on the critical spheres. Then the inverse images of the two curves are diffeomorphic if their associated configurations of labeled critical points are equivalent.*

REMARK 7.3: It is clear that one does not actually need the endpoints of the two curves to be equal, merely that they lie in the interiors of the same annular regions between adjacent critical radii.

DEFINITION 7.4: *A curve γ is monotone if the associated ordered sequence of critical radii is monotone.*

In the case of monotone curves, in order to understand the diffeomorphism type of the associated inverse image, it is sufficient to assume that the curve is a segment of a ray from the origin, and we will concentrate on *monotone curves* - and consequently, segments on rays from the origin - in what follows.

EXAMPLE 7.5: Suppose that the base is a prismatic joint, which, for simplicity, we will assume simply means that the length of the base varies in the closed interval $[l_n(0), l_k(1)]$. *Then the resulting configuration space will be the inverse image of the line segment*

$$[l_k(0), l_k(1)]$$

along the positive x-axis.

EXAMPLE 7.6: Suppose that we are interested in the inverse image of l_n along the x-axis, and suppose that l_k is not a critical radius. Then the configuration space $\mathcal{C}(l_1, \ldots, l_k)$ is non-singular and is the boundary of the inverse image of the segment $[l_m, l_1 + l_2 + \cdots + l_k]$.

Likewise, the union of the configuration spaces $\mathcal{C}(l_1, \ldots, l_k(0))$ and $\mathcal{C}(l_1, \ldots, l_k(1))$ is the boundary of the configuration space described in 7.5.

EXAMPLE 7.7: When we bootstrap in the plane, and construct the configuration space

$$\mathcal{C}(l_1, \ldots, l_k)$$

by taking the inverse image of the intersection of the circle centered at l_k of radius l_1 with the free workspace for $(l_2, \ldots, l_{k-1})$ we break the intersection up into two pieces, the inverse image of the part of the circle above the x-axis and the inverse image of the part of the circle below it. Both of these are monotone and consequently diffeomorphic. We have just proved the following theorem:

THEOREM 7.8: *The configuration space of a closed chain in $\mathbb{R}^2$ is the double over the boundary of the inverse image of a monotone path and hence a segment along the x-axis.*

REMARK: Bootstrapping in $\mathbb{R}^n$ involves the inverse image of the intersection of a sphere S^{n-1} with the workspace. This inverse image also breaks up into a union over the common boundary of two diffeomorphic pieces, one corresponding to the upper hemisphere and one to the lower. The distinction is that our techniques only enable us to identify the inverse images of curves γ and so the exact structure of these inverse images for $n > 2$ are not really available in this way. However, by using curves in the image of the configuration space for all k links we are able to determine these spaces explicitly, though this does not give them as explicit doubles.

§8: The homotopy types of the inverse images of curves

In §7 we reduced the analysis of the homotopy for the inverse image of any C^∞ curve in the workspace to the study of the inverse images of straight line segments. In this

section we consider the inverse image of the line segment S along the x_1-axis from $l > 0$ to $\sum l_i$, the radius of the workspace, *where l is not a critical value.* For convenience set E_x to be the unit vector contained in S, the unit vector pointing in the positive x_1-direction.

$$E_x \;=\; \begin{pmatrix} 1 \\ 0 \\ \vdots \\ 0 \end{pmatrix}.$$

Suppose that $r_I \in S$, is a critical radius. Note that if I' is the set of j, $1 \le j \le k$ with $j \notin I$ then $r_{I'} = r_I$. To choose between them, we note that

$$\sum_{i \in I} -l_i + \sum_{j \notin I} l_j = -\left(\sum_{s \in I'} -l_s + \sum_{w \notin I'} l_w \right) \neq 0$$

so only one choice of signs gives a positive signed sum. In the rest of this section, we assume that the signed sum for I is the positive one. Consequently, for each I with critical radius r_I contained in S we have.

8.1
$$\sum_{i \notin I} l_i - \sum_{j \in I} l_j = r_I > 0,$$

For each $j \in I$, the j-interval is parallel to the x_1-axis and points inward.

For each such I we denote by T^I the subspace $(S^{n-1})^{|I|}$ contained in the configuration space defined by setting the unit vectors which are not in I to be E_x, while freely varying the links with $i \in I$. The image of the endpoint map e on T^I is an annulus or an n-ball centered about the point $\sum_{i \notin I} l_i E_x$ having outer radius $\sum_{i \in I} l_i$.
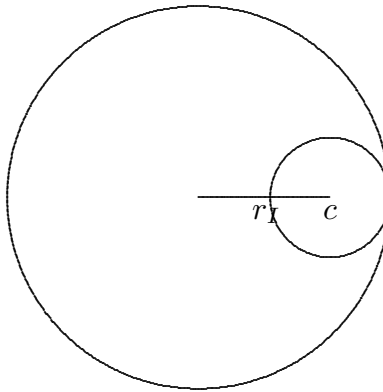

Figure 11: $c = \sum_{i \notin I} l_i$

Thus, to each critical value r_I in S there is associated a unique sub-coordinate product $(S^{n-1})^{|I|}$ in the total configuration space $(S^{n-1})^k$, and these T^I fit together in the sense

21

that if $J \subset I$, then $r_J \in S$ and then $T^J \subset T^I$. Conversely, for each coordinate sub-product $(S^{n-1})^m$ contained in T^I there is a unique J so this sub-product is T^J.

DEFINITION 8.2: *The union of these T^I, $e_I \in S$, is written X_S.*

As constructed, X_S does not lie in $e^{-1}(S)$. In fact, all that we can say about X_S at this point is that

(8.3) $e(X_S)$ is entirely contained in the positive half-ball of the workspace, that is to say, the region consisting of all points with positive first coordinate, $x_1 > 0$.

(8.4) The integral homology of X_S is torsion free, has one generator for each $r_I \in S$ (in dimension $|I|(n-1)$) and injects into the homology of the entire configuration space.

(For 8.4 note that X_S is a sub-complex of the CW-complex $(S^{n-1})^k$ where S^{n-1} is given as a cell complex having a single 0-cell, $e_0 = E_x$, and a single $(n-1)$-cell, while $(S^{n-1})^k$ is realized as the product CW-complex. We now indicate how to construct a deformation of X_S to a sub-complex of $e^{-1}(S)$.)

Recall the definition of the action $SO_n \times (S^{n-1})^k \longrightarrow (S^{n-1})^k$ defined in 6.3.

LEMMA 8.5: *There is a continuous map $h: I \times X_S \longrightarrow SO_n$ satisfying $h|0 \times X_S$ is the identity in SO_n, so that the one parameter family of embeddings*

$$P_t: X_S \longrightarrow (S^{n-1})^k$$

defined by $P_t(v) = h(t, v)(v)$, satisfies $P_1(v) \in e^{-1}(S)$ for all $v \in X_S$.

PROOF: The fibration,

8.6
$$
\begin{array}{ccc}
SO_{n-1} & \longrightarrow & SO_n \\
 & & \downarrow {\scriptstyle Eval} \\
 & & S^{n-1}
\end{array}
$$

where $Eval(g) = g(E_x)$ for $g \in SO_n$, is trivial over $S^{n-1} - (-E_x)$. Consequently, there is a C^∞ lifting $L: S^{n-1} - (-E_x) \longrightarrow SO_n$ so that

(1) $Eval \cdot L = Id$,

(2) $L(E_x) = Id \in SO_n$.

For an explicit lifting see, e.g., [ST].

For any point $v \in X_S$, $e(v)$ is in the positive half-ball, and, in particular $e(v) \neq 0$. The unit vector from the origin pointing in the direction of $e(v)$ consequently lies in

$S^{n-1} - (-E_{x_1})$. Moreover, there is a unique geodesic in $S^{n-1} - (-E_{x_1})$ between this unit vector and E_{x_1}. Using these geodesics we obtain, in the obvious way, a map $\lambda \colon I \times X_S \to S^{n-1} - (-E_{x_1})$, so that $\lambda(1, v)$ is the unit vector in the direction of $e(v)$ and $\lambda(0, v) = E_{x_1}$.

The map h in 8.5 is now defined as

$$h(t, v) = (L \circ \lambda(t, v))^{-1}.$$

∎

COROLLARY 8.7: $e^{-1}(S)$ is homotopy equivalent to X_S and is tautly embedded in $(S^{n-1})^k$ in the sense that the integral homology of $e^{-1}(S)$ embeds into the integral homology of $(S^{n-1})^k$ as a direct summand.

PROOF: We have constructed an embedding of X_S in $e^{-1}(S)$, and a homotopy of this embedding to a CW-embedding of X_S as a sub-complex of the usual cellular decomposition of $(S^{n-1})^k$. Moreover, the integral homology of $e^{-1}(S)$ generated by these cells forms a direct summand of $H_*(e^{-1}(S), \mathbb{Z})$. Consequently, we have shown that every cell of $X_S \subsetneq e^{-1}(S)$ is essential. On the other hand, there are exactly as many cells in X_S as there are critical points in $e^{-1}(S)$ for the Morse function discussed in 6.6. Hence, we have accounted for all the cells needed to construct $e^{-1}(S)$, and 8.7 follows. For $n > 2$ it follows that there are no one cells in the decomposition, and the fundamental group $\pi_1(e^{-1}(S)) = \{1\}$. Consequently, the homology isomorphism gives a homotopy equivalence using the Whitehead theorems. When $n = 2$ we have to be a little more careful. Note that we can extend the embeddings constructed in this section to embeddings of the normal bundles to the products of spheres, $(S^{n-1})^l$, as open neighborhoods in $e^{-1}(S)$. (In the next section we will show that these normal bundles are actually trivial but we don't need this here.) Since each of these products of spheres contains exactly as many critical points as the sum of the dimensions of the homology groups of $(S^{n-1})^l$, the same is true for the embedded normal bundle provided we make it sufficiently small.

The Morse flow associated to the Morse function can be assumed to stay within this neighborhood in a sufficiently small neighborhood of the key critical point. Then, by induction, one can argue that the attaching map of this top cell is the usual one, attaching it as the top cell of the product of S^{n-1}-spheres. This completes the proof. ∎

REMARK 8.8: It follows from 8.7 that the cohomology map

$$H^*((S^{n-1})^k, \mathbb{Z}) \to H^*(e^{-1}(S), \mathbb{Z})$$

is surjective (and explicit). Consequently, the cup-products in $H^*(e^{-1}(S), \mathbb{Z})$ are entirely determined.

§9: The normal neighborhoods of the $T^I \subset e^{-1}(S)$.

As we have noted in 8.3, the unit vector from the origin in the direction of any point in $e(X_S)$ always lies in the open right hemisphere. Hence, since X_S is compact, there is an $\epsilon > 0$ so that this statement remains true if, instead of taking

$$\left(\sum_{j \notin I} l_j\right) E_x + \sum_{i \in I} l_i X_i$$

to define our interior n-ball or annulus, we take the sum

9.1
$$\left((\sum_{j \notin I} l_j) - t\right) E_x + \sum_{i \in I} l_i X_i$$

for $0 \leq t \leq \epsilon$ to define a new interior n-ball or annulus.

Now we restrict attention to just the links in the set $J = \{i \mid i \notin I\}$, and consider the end-point map on their configuration space $(S^{n-1})^{|J|}$. Let $R = \sum_{j \in J} l_j$ be the radius of the image of this end-point map. Let $\gamma_J \subsetneq$ the n-ball of radius R be the path

9.2
$$\begin{pmatrix} R - t \\ 0 \\ 0 \\ \vdots \\ 0 \end{pmatrix}$$

for $0 \leq t < \epsilon$ with ϵ satisfying the condition above and also the condition that γ only intersects the single singular image sphere of radius R. Since $e^{-1}(\gamma_J)$ contains only a single critical point, a maximum, it is a ball of dimension $(n-1)(|J| - 1)$, $D^{(n-1)(|J|-1)}$. Consequently we have an explicit embedding

$$h_I \colon M_I(T^I) \ \cong \ D^{(n-1)|J|} \times T^I \subset (S^{n-1})^k.$$

This embedded set has codimension $(n - 1)$, so it is not open. But this is exactly the codimension of $e^{-1}(S)$ in $(S^{n-1})^k$, so if it were to be contained in $e^{-1}(S)$ it would be open there.

Let P_I the the composition $e \circ h_I$.

$$P_I \colon D^{(n-1)(|J|-1)} \times S^{(n-1)|I|} \longrightarrow \mathbb{R}^n.$$

It's image is contained entirely in the subspace of image e with $x_1 \geq \tau$ for a $\tau > 0$. Consequently, the map π_I from $Im(P_I)$ to S^{n-1} obtained by taking the unit vector in the direction of the line from the origin to $P_I(w)$ for each $w \in M_I(T^I)$, is contained in $S^{n-1} - (-E_x)$, and we have a well defined map

$$\lambda \colon M_I(T^I) \longrightarrow SO_n$$

defined as the composition $L \circ \pi_I$. As was the case with 8.5 we have

LEMMA 9.3: *The map*

$$\Lambda \colon M_I(T^I) \longrightarrow (S^{n-1})^k$$

defined by $\Lambda(w) = \lambda(w)^{-1} P_I(w)$ *is a differentiable embedding* $M_I(T_I) \subset e^{-1}(S)$.

This establishes the fact that the normal bundle to T^I in $e^{-1}(S)$ is trivial. The next thing to check is how two different T^I and $T^{I'}$ intersect the normal bundle to $T^{I \cap I'}$.

LEMMA 9.4: *Let* $I'' = I \cap I'$, *so we have*

$$T^I \cap T^{I'} \;=\; T^{I''}.$$

The following statements hold.

9.5 $I \cup I' \neq \{1, 2, 3, \ldots, k\}$.

9.6 Let

- $K_1 = I - \{I \cap I'\}$,

- $K_2 = I' - \{I \cap I'\}$,

- K_3 *be the compliment of* $I \cap I'$ *in* $\{1, 2, \ldots, k\}$.

Then we can choose coordinates for the disk $e^{-1}(\gamma_{I \cap I'})$ *in a sufficiently small neighborhood of the point where all the vectors are equal so that the coordinates corresponding to* $K_1 \cup K_2$ *are part of the coordinate set.*

For 9.5 note that $\sum_1^k l_j - 2 \sum_{i \in I} l_i > 0$ and $\sum_1^k l_j - 2 \sum_{m \in I'} l_m > 0$. If $I \cup I' = \{1, \ldots, k\}$, then both the above equations cannot hold simultaneously. Thus $I \cup I' \neq \{1, \ldots, k\}$.

For 9.6 note that 9.5 implies that $K_1 \cap K_2 = \emptyset$ and $K_1 \cup K_2 \subsetneq K_3$. Let $v \in \{1, \ldots, k\}$ be contained in $K_3 - (K_1 \cup K_2)$. Let γ be the curve 9.2 for K_3. Then γ has codimension $(n-1)$ in the workspace so it is determined in a perhaps smaller neighborhood of the extremal point $\sum_{j \in K_3} l_j E_{x_1}$ by making an arbitrary single coordinate a function of the remaining coordinates. In particular, we can choose this coordinate to be the one corresponding to v. So 9.6 follows. ∎

Let $K_4 = \{1, \ldots, k\} - I$ and let $K_5 = \{1, \ldots, k\} - I'$. Both T^I and $T^{I'}$ contain $T^{I \cap I'}$, but it is not true that $M_I(T^I)$ and $M_{I'}(T^{I'})$ are contained in $M_{I \cap I'}(T^{I \cap I'})$. We now want to discuss the way that the normal bundles to the two products T^I and $T^{I'}$ fit together in a neighborhood of $T^{I \cap I'}$.

THEOREM 9.7: *Let $M_{I \cap I'}(T^{I \cap I'}) = T^{I \cap I'} \times \mathbb{R}^{K_1} \times \mathbb{R}^{K_2} \times \mathbb{R}^{K_4 \cap K_5}$ where the factors $\mathbb{R}^{K_1}$ and $\mathbb{R}^{K_2}$ are the coordinate planes of 9.6. Then the normal bundles $N_{T^I}(T^{I \times I'})$ and $N_{T^{I'}}(T^{I \times I'})$ span $\mathbb{R}^{K_3} \times \mathbb{R}^{K_4}$ at every point of $T^{I \cap I'}$.*

PROOF: Let V be a small neighborhood of $T^{I \cap I'}$ in T^I. Then the composition

$$(\Lambda)^{-1} \circ P_1 : V \longrightarrow M_{I \cap I'}(T^{I \cap I'})$$

defined using Λ from 9.3 and P_1 from 8.5 is what one expects on $T^{I \cap I'}$ but is not quite expected on $V - T^{I \cap I'}$. Thus, on coordinates associated to K_1 the X_j are close to E_{x_1}, but on K_4 coordinates, all the X_v are equal, but not necessarily equal to E_{x_1}, since we must have

$$\sum_{j \in K_1} l_j X_j \oplus \left(\sum_{v \in K_4} l_v \right) X_{v_0} = t E_{x_1},$$

for some positive value of t. Thus we can give coordinates for this region as the X_j, $j \in K_1$, with the elements in K_2 and $K_4 - K_2$ determined via the equations

$$\sum_{i \in K_1} l_i X_i + \left(\sum_{j \in K_4} l_j \right) X_{v_0} = t E_{x_1}.$$

Consequently, the τ coordinate in X_{v_0} is given as

$$\frac{-1}{\sum_{j \in K_4} l_j} \sum_{1 \in K_1} l_i X_{i,\tau}, \ 2 \le \tau \le n,$$

and we have

$$\frac{\partial X_{v_0, \tau}}{\partial X_{i, \tau}} = \frac{-l_i}{\sum_{j \in K_4} l_j}.$$

Let $A_1 = \sum_{i \in K_1} l_i$, $A_2 = \sum_{j \in K_2} l_j$ and $A_3 = \sum_{w \in K_3} l_w$. Then the Jacobian for the embeddings of the two normal bundles to $T^{I \cap I'}$ in T^I and $T^{I'}$ has the form

9.8
$$\begin{pmatrix} I & N \\ N' & I \end{pmatrix}$$

where the general form of N is $(n-1)$ equal diagonal blocks, (one for each τ). Each diagonal block has the form

$$N = \frac{-1}{A_2 + A_3} \begin{pmatrix} l_{i_1} & l_{i_1} & \cdots & l_{i_1} \\ \vdots & \vdots & \ddots & \vdots \\ l_{i_r} & l_{i_r} & \cdots & l_{i_r} \end{pmatrix}$$

26

where $i_1, \ldots i_r$ are the coordinates in K_1. There is a similar description for N'. It contains $(n-1)$ diagonal blocks, each of the form

$$N' = \frac{-1}{A_1 + A_3} \begin{pmatrix} l_{j_1} & l_{j_1} & \cdots & l_{j_1} \\ \vdots & \vdots & \ddots & \vdots \\ l_{j_s} & l_{j_s} & \cdots & l_{j_s} \end{pmatrix}$$

where $K_2 = \{j_1, \ldots, j_s\}$. The determinant of the matrix in 9.8 is the same as the determinant of $I - NN'$ where NN' is a square matrix consisting of $(n-1)$ diagonal blocks, each of the form

$$NN' = \frac{A_2}{(A_2 + A_3)(A_1 + A_3)} \begin{pmatrix} l_{i_1} & l_{i_1} & \cdots & l_{i_1} \\ \vdots & \vdots & \ddots & \vdots \\ l_{i_r} & l_{i_r} & \cdots & l_{i_r} \end{pmatrix}.$$

Since each diagonal block in NN' has rank 1 we directly calculate that the determinant is

$$\left(1 - \frac{A_1 A_2}{(A_1 + A_3)(A_2 + A_3)} \right)^{n-1},$$

but this is

$$\left(\frac{A_3(A_1 + A_2 + A_3)}{(A_1 + A_3)(A_2 + A_3)} \right)^{n-1}$$

and is always non-zero. ∎

COROLLARY 9.9: *Given any two tori T^I and $T^{I'}$ in $e^{-1}(S)$, if $T^{I \cap I'}$ is the intersection torus, then locally the union $M(T^I) \cup M(T^{I'})$ is obtained via a plumbing construction where an appropriate collection of normal coordinates to T^I over $T^{I \cap I'}$ are identified with the usual coordinates in $T^{I'}$.*

REMARK 9.10: When T^I and $T^{I'}$ have complementary dimensions then they intersect in the single point where all the links point in the same direction. Thus, their cap product will be 1.

Bibliography

[A] J.F. Adams, On the non-existence of elements of Hopf invariant one, *Ann. Math.*, **72**(1960), 20-104.

[C] J. F. Canny, *The Complexity of Robot Motion Planning*, Thesis, MIT, 1987.

[Ha] J.-C. Hausmann, Sur la topologie de bras articulès, *Algebraic Topology Poznań 1989*, 146-159, *Lecture Notes in Math.*, 1474 Springer, Berlin, 1991

[HK] J.-C. Hausmann, A. Knutson, The cohomology ring of polygon spaces, *Ann. Inst. Fourier (Grenoble)*, **48** (1998), 281-321.

[H] K.H. Hunt, *Kinematic Geometry of Mechanisms*, Oxford University Press, 1978.

[K1] Y. Kamiyama, Topology of equilateral polygon linkages, *Topology and its Applications*, **68**(1996), 13-31.

[K2] Y. Kamiyama, Chern numbers of the moduli space of spatial polygons, *Kodai Math. J.*, **23**(2000), 380-390.

[K3] Y. Kamiyama, Euler characteristic of the moduli space of polygons in higher-dimensional Euclidean space, *Kyushu J. of Math.*, **54**(2000), 333-369.

[KTT] Y. Kamiyama, M. Tezuka, T. Toma, Homology of the configuration spaces of quasi-equilateral polygon linkages, *Trans. AMS*, **350**(1998), 4869-4896.

[KT] Y. Kamiyama, M. Tezuka, Topology and geometry of equilateral polygon linkages in the Euclidean plane, *Quart. J. Math.*, **50**(1999), 463-470.

[KM1] M. Kapovich, J. Millson, On the moduli spaces of polygons in the Euclidean plane, *Journal of Diff. Geometry*, **42** (1995), 133-164.

[KM2] M. Kapovich, J. Millson, The symplectic geometry of polygons in Euclidean space, *Journal of Diff. Geometry*, **44** (1996), 479-513.

[KM3] M. Kapovich, J. Millson, Universality theorem for configuration spaces of planar linkages, *Preprint, U. of Utah*, (1998).

[KLOS] L.E. Kavraki and P. Švestka and J.-C. Latombe and M.H. Overmars, Probabilistic Roadmaps for Path Planning in High-Dimensional Configuration Spaces", *IEEE Transactions on Robotics and Automation*, **12**, (1996), 566–580.

[SM] G. Shukla and A.K. Mallik, Detection of a crank in six-link planar mechanisms, *Mechanism and Machine Theory*, **35**, (2000), 911–926.

[ST] D.B.A Epstein, N.E. Steenrod, *Cohomology Operations*, Annals of Mathematics Studies # 50, Princeton University Press.

[WXH] P. Watterberg, P.Xavier and Y. Hwang, Path Planning for Everyday Robotics, *icra*, (1997), 1170–1175.